

Dynamic Analysis and Experimental Evaluation of Variable Valve Lift System for Internal Combustion Engine with Double Overhead Camshaft

Saeed A. Albatlan^a and Eid S. Mohamed^b

^aAutomotive Engg., Higher Technological Institute,
6th of October City Campus, Egypt.
Corresponding Author, Email: saeedzeed@yahoo.com

^bAutomotive and Tractors Engg.,
Helwan University, Mataria, Cairo, Egypt.
Email: eng_eid74@yahoo.com

ABSTRACT:

In modern four-stroke automobile engine technology, variable valve timing and lift control offer potential benefits for making a high performance engine. Variable valve lift (VVL) system for automotive engines is one of the key technologies to attain improvement of fuel economy, power output and reduction of emission. This paper describes an analytical simulation model of the VVL system. The VVL mechanism with a polynomial cam profile is designed to have maximum lift that is greater than the lift of the conventional mechanism. A dynamic model of VVL mechanism with three degrees of freedom is presented. The N42-BMW cylinder head with Valvetronic VVL of internal combustion engine was used in the test set-up. The motored cylinder head test data focuses on VVL system response and evaluation of the developed VVL mechanism. The performance results of a VVL for an overhead camshaft were investigated on the basis of theoretical simulation and experimental data to verify the validity of the VVL system in the test rig.

KEYWORDS:

Variable valve lift; Dynamic model; Valvetrain; Engine Valvetronic; Multibody dynamics; Valve lift regulation

CITATION:

S.A. Albatlan and E.S. Mohamed. 2014. Dynamic Analysis and Experimental Evaluation of Variable Valve Lift System for Internal Combustion Engine with Double Overhead Camshaft, *Int. J. Vehicle Structures & Systems*, 6(1-2), 24-31. doi:10.4273/ijvss.6.1-2.04

ACRONYMS & NOMENCLATURE:

VVL	Variable Valve Lift
VVT	Variable Valve Timing
DC	Direct Current
IC	Internal Combustion
DOHC	Double Over Head Camshaft
EGR	Exhaust Gas Recirculation
RFF	Roller Finger Follower
VVA	Variable Valve Actuation
CVVL	Continuously Variable Valve Lift
rpm	Revolutions Per Minute
S_h	Follower lift, mm
ω	Angular speed, rpm
v	Follower velocity, m/s
a	Follower acceleration, m/s ²
h_{max}	Maximum follower lift, mm
C, C^*	Design constants
F_{ir}	Rocker arm equivalent inertia force, N
F_{iv}	Valve equivalent inertia force, N
m_v, m_f	Valve and follower masses, kg
I	Rocker arm moment of inertia, kg m ²
α_r	Angular acceleration of rocker arm, rad/s ²
F_n	Normal force, N
F_c	Contact force, N
ϕ	Pressure angle, degree
μ	Friction coefficient
K_s	Spring stiffness, N/m

1. Introduction

Many factors have to be taken into account in the design of motor engine valvetrains and cams, which may be briefly classified into fluid dynamics and mechanical ones. The maximum lift and timing of valve are determined based on fluid dynamics. Efforts should be minimized to work within the allowable stress levels and loss of contact between cam and follower should be avoided. Complexity appears because of nonlinearities introduced by the kinematic chain between the cam and valve. There are many works done in the design of cam, valve and the whole mechanical valve chain. The current methodology enables the design of valvetrain systems. The desire for optimum fuel economy, improved performance and drive expectations of customers are gradually increasing along with stringent emission regulations set by the government. Many original engine manufacturing companies are prompted to consider the application of high function variable valve actuation (VVA) mechanisms in their vehicles as a solution. The VVA is a mechanism that can alter the shape or timing of a valve lift event within an internal combustion (IC) engine. It allows the lift and timing in various combinations of the intake and exhaust valves to be changed while the engine is in operation.

Variable Valve Timing (VVT) and Variable Valve Lift (VVL) are designed to overcome the limitation of having a fixed opening period and valve lift throughout the engine's speed range. The optimization of cylinder breathing is difficult in modern car engines since they operate over a wide range of speed from 1000 to 6000 rpm. In the low-to-mid speed range, the engine performs better and the emission levels are lower if the intake valves open late and close relatively early. The low lift assists in better atomization of charge at lower velocities of flow. Conversely, at high engine speed, the cylinder breathing is improved by opening intake valve slightly earlier and closing late to make use of the ram momentum effect. The high lift helps the engine to induct more air during suction. However, in fixed valve timing and lift, the engine performance is optimized in the mid-speed range at the expense of performance below optimum at low and high engine speeds [1].

VVL mechanisms provide two lift profiles, which have been used by vehicle manufacturers for many years. They have shown fuel economy, performance and emission improvements. The evolution of VVL from two or three fixed lifts to continuously variable valve lift (CVVL) provides a significantly larger family of lift profiles. CVVL systems permit engine throttling through valve lift adjustments to further minimize the pumping losses. Several vehicle manufacturers are evaluating the benefits of CVVL mechanisms to improve the efficiency while providing engine power that customers are demanding [7, 8]. To extract the maximum fuel economy benefit, the following criteria must be met:

1. The engine must operate un-throttled;
2. The CVVL mechanism must provide sufficient valve lift to avoid significant pressure loss across the valve at peak intake flow;
3. Engine operation near the dilution limit must be maintained.

The first two criteria ensure that pumping losses are minimized, while the third criterion maximizes the gross indicated efficiency. However, best efficiency generally occurs using a small amount of throttling. The CVVL mechanism must be driven through a cam phaser having sufficient power to close the intake valve at the point required to produce the desired load, while also advancing Intake Valve Opening (IVO) to the point required to place the engine at its dilution limit using internal residual. The task is to determine the lift profile and IVO required for maximizing the thermal efficiency at each of the four test points [3].

VVL mechanism offers best fuel economy, reduces NO_x gas and increases the peak torque and power. A number of investigations related with the VVL mechanism have been reported. Since the intake and exhaust valve timings provide the best fuel economy, idle stability and highest power change according to the engine operating zone, a VVT system is very beneficial. In most of the current electro-hydraulic valvetrains, the valve displacement is controlled by the high pressure spool valve opening interval. Anderson et al. [11] designed an adaptive pole placement controller based on the simplified system model to control the maximum lift. They controlled the pulse-width of the signal transmitted to the high pressure solenoid valve to adjust the

hydraulic flow to the engine valve actuator for controlling the engine valve lift within each cycle. A combination of adaptive feed forward and feedback controllers were employed to control the engine valve displacement. A non-linear inverse model of the system was developed to design the feed forward controller. The valve displacement, hydraulic supply pressure and the spool-valve position were measured precisely as feedback signals to the controller [4].

In this paper, a dynamic model of VVL mechanism for four-cylinder engine Valvetronic using three degrees of freedom is developed. The performance of the designed VVL mechanism is then studied through simulations and experimental tests.

2. VVL principle

The Valvetronic VVL control system incorporates an electrically adjustable arm to control the maximum lift of inlet valve as camshaft rotates. In this way, Valvetronic controls the lift of the inlet valve. The volume of inducted air as a function of engine speed exhibits:

- a. Valve lift is maximum when the engine is revolving at high speed and the valves open fully in order to ensure rapid charging of the combustion chambers;
- b. Valve lift at low engine speeds is minimal. Less fuel-air mixture can make its way into the cylinder.

The VVL mechanism employs shaft mounted input and output rocker arms in between a conventional cam shaft and roller finger followers (RFF) as shown in Fig. 1. A rotating control shaft is used to orient the cam surface of the output rocker relative to RFF rollers. Control shaft is eccentrically mounted on shaft supports which attach the VVL mechanism to the cylinder head. Eccentric bushings mounted on the control shaft form the center of rotation of input rockers. Cylindrical pallet interface transmits the motion from the input to the output rocker while allowing relative motion when the centers of rotation are not concentric. Eccentric mounting of the control shaft and input rocker bearing are oriented such that they are coincident at full lift.

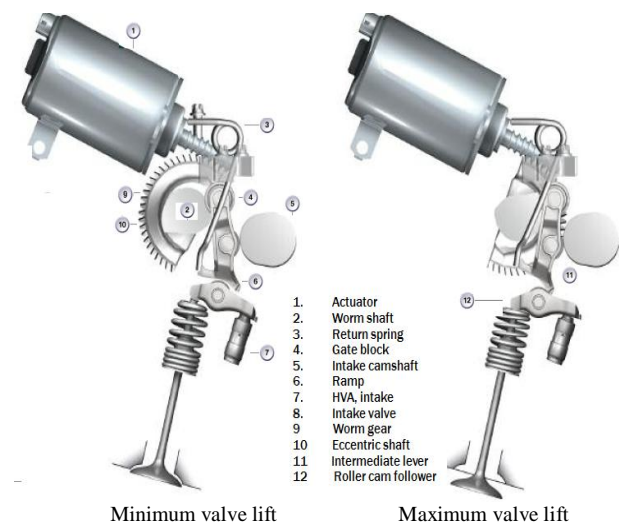


Fig. 1: Valvetronic VVL control system [3]

The intermediate lever varies the transmission ratio between the camshaft and RFF. The valve lift (10 mm) and opening time are at a maximum for the full load

position. The valve lift (0.2 mm) and opening time are set to minimum in the idling position. The roller cam followers and associated intermediate levers are divided into four classes. A corresponding code number is punched on the components. They always have the same class per pair. Assignment of the roller cam followers and the intermediate levers at the production plant ensures that the cylinders are uniformly charged even at the minimum valve lift of 0.2 mm [3, 9].

3. Theoretical analysis

3.1. Cam profile and follower motion

Modern tractor and automobile engines employ polynomial cam for valve opening and closing over a wide ranges of engine speed. Valves allow air/fuel mixture to enter into the cylinder compartment and the residue to leave the cylinder's compartment after one combustion cycle of a cylinder has been completed. A cam pushes against a valve so that it can be opened when the camshaft is rotated to its specific profile. A spring located on top of the valve returns it to the closed position. The study began with the implementation of a numerical procedure specifically designed to determine the cam profile, kinematic and dynamic characteristics of the whole system. Rocker arm geometry, relative positions and inertial data of elements, spring stiffness, preloading, camshaft speed and valve lift law were used as inputs. The model was validated against the conventional timing system using kinematic simulations.

The model gives a smooth curve for fundamental valve lift as well as to its higher derivatives. The use of a polynomial order greater than 8 might cause a dramatic change in the system behaviour with the addition of system constraints on the motion of the cam follower including the lift displacement, velocity and acceleration. In this analysis, the system is modelled and analyzed for the given constraints and is then perturbed to examine the effect on the system stability [10]. The follower displacements may be expressed in terms of polynomial as follows:

$$S_h = h_{\max} \left[1 + C \left(\frac{\theta}{\beta} \right)^2 + C_p \left(\frac{\theta}{\beta} \right)^p + C_q \left(\frac{\theta}{\beta} \right)^{p+2} + C_r \left(\frac{\theta}{\beta} \right)^{p+4} \right] \quad (1)$$

$$v = \frac{ds}{dt} = \omega \frac{ds}{d\theta} \quad (2)$$

$$a = \frac{d^2s}{dt^2} = \omega^2 \frac{d^2s}{d\theta^2} \quad (3)$$

Where S_h refers follower lift. ω is angular speed. v and a are velocity and acceleration of follower. h_{\max} is maximum follower lift. The design constants C , C_p , C_q , C_r are defined as follows:

$$C = \frac{-6p^2 - 24p}{6p^2 - 8p - 8}, C_p = \frac{p^3 + 7p^2 + 14p + 8}{6p^2 - 8p - 8} \quad (4)$$

$$C_q = \frac{-2p^3 - 4p^2 + 16p}{6p^2 - 8p - 8}, C_r = \frac{p^3 - 3p^2 + 2p}{6p^2 - 8p - 8}$$

3.2. Valvetrain kinematics

The actuation forces on the follower are the inertia, spring and frictional forces. Any reciprocating mass of

the valvetrain produces cyclic inertia forces as shown in Fig. 2. Positive inertia forces are regarded as those which tend to press the cam follower onto the cam flank. Negative inertia forces tend to separate the cam and follower. Negative forces are the critical forces, as they must be opposed by the valve return-springs. If these negative inertia forces are large, stiff return-springs will become necessary to counteract the undesirable jump-off response. Unfortunately, the same spring load is added to the inertia load during periods of positive acceleration and deceleration. This will increase the cam and follower stress and accordingly will cause high wear and damage to the cam flanks and follower. The valvetrain inertia forces are given by,

$$F_{Inertia} = F_{iv} + F_{ir} + F_{if} \quad (5)$$

$$F_{iv} = m_v * a = m_v \frac{d^2s}{dt^2} = m_v \omega^2 \frac{d^2s}{d\theta^2} \quad (6)$$

$$F_{ir} = \frac{Ja}{L_r^2 \cos\beta} = \frac{J\omega^2}{L_r^2 \cos\beta} \frac{d^2r}{d\theta^2} \quad (7)$$

$$F_{if} = m_f * a = m_f \frac{d^2s}{dt^2} = m_f \omega^2 \frac{d^2s}{d\theta^2} \quad (8)$$

Where F_{ir} is equivalent inertia force of RFF. F_{iv} is valve equivalent inertia force. m_v and m_f are valve and follower masses. J is moment of inertia of RFF. L_r is rocker arm linkage from pivot point to center of follower. α_r and α are the angular acceleration of rocker arm and cam respectively.

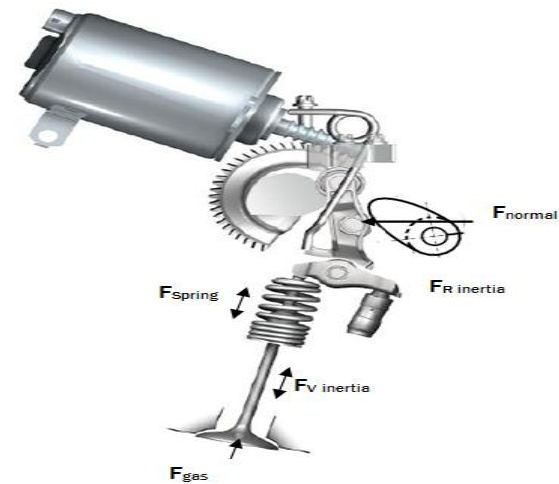


Fig. 2: Forces acting on VVL

The valve spring force is given by,

$$F_s = F_{st} + F_{dy} \quad (9)$$

The static valve spring force F_{st} is obtained by multiplying the spring rate by the deflection of the spring from its installed height and adding any preload. The deflection of the spring at any point in the cycle is equal to the valve lift and is governed by,

$$F_{st} = k * \delta_o + k * S_h \quad (10)$$

Where δ_o is spring compression at start of lift. k is spring stiffness. The dynamic spring force F_{dy} is defined as the force obtained from the valve spring when it is operating at a given frequency and varies considerably from the

static force at high operating frequencies. The dynamic valve force F_{dy} is given by [14]:

$$F_{dy} = F_{initial} + 180 * k * \omega \left[\sum dl_v / d\theta \right] / f_N \quad (11)$$

Where $F_{initial}$ is preload force exerted by valve spring at its installed height. f_N is natural frequency of the valve spring. The friction force (F_f) acts on the follower in the same direction as the cam rotates against the follower and is derived as,

$$F_f = \mu(F_n \sin\phi) \quad (12)$$

Where ϕ is pressure angle. μ is friction coefficient that is negative for $\phi < 90$ and is positive for $\phi > 90$. The normal force (F_n) can be evaluated using,

$$F_n = F_c = \frac{[F_s + F_{iv} + F_g] \frac{L_r}{L} + [F_{ir} + F_{if}]}{[\cos\phi - \mu * \sin\phi]} \quad (13)$$

3.3. Valvetrain dynamic model

The arrangement of a single valvetrain VVL mechanism can be modelled as a multibody system, comprising a number of mass elements which are connected to each other by a series of restraining elements. These elements represent the sources of compliance in the system, such as the valve spring stiffness and contact compliance between the cam and the RFF. The inertial properties of the mechanism, springs and dampers account for the system stiffness and damping. A constrained inertial dynamic model incorporating the elastic behaviour of various valvetrain elements is required. Each component contributes to the system dynamics through its stiffness and damping properties. Special care is taken while modelling the contact conditions. Fig. 3 is a schematic representation of the equivalent valvetrain mechanism as a two-mass system model with three degrees of freedom.

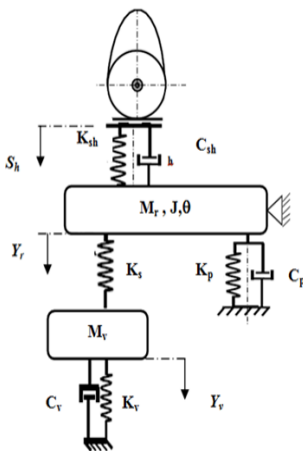


Fig. 3: Dynamic model of VVL

Two lumped mass elements (valve m_v , RFF m_r) are considered to be rigid representing the mass of several components of the valvetrain system. The cam shoe connects to mass m_v through a spring K_v and damper C_v . Mass m_r is mounted by a return spring stiffness K_s and hydraulic latch plunger damper and stiffness C_p and K_p . Applying Newton's second law of motion:

$$M_v \ddot{Y}_v = K_v(Y_v) + C_v(\dot{Y}_v) - K_s(Y_r - Y_v) \quad (14)$$

$$M_r \ddot{Y}_r = K_s(Y_r - Y_v) - C_{sh}(\dot{S}_h - \dot{Y}_r) - K_{sh}(S_h - Y_r) + C_p(\dot{\delta}) + K_p(\delta) + F_C \quad (15)$$

$$J_r \ddot{\theta} = C_{sh} L_r^2 (\dot{S}_h - \dot{Y}_r) + L_r K_{sh} (S_h - Y_r) - L_r K_s (\theta) - M_F \quad (16)$$

The equations of motion of the valvetrain system have been derived by applying Lagrange's energy approach, and formulated in matrix form as follows:

$$[M]\{\ddot{X}\} + [C]\{\dot{X}\} + [K]\{X\} = \{F\} \quad (17)$$

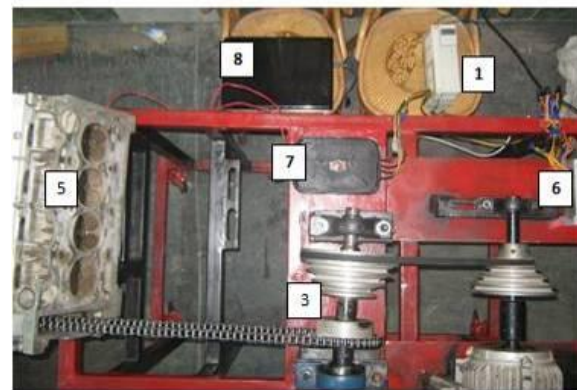
$[M]$, $[C]$ and $[K]$ are mass, damping and stiffness matrices related to the rigid body modes of the vehicle system. The contact force acting on the cam is given by,

$$F_C = C_{sh}(\dot{S}_h) + K_{sh}(S_h) \quad (18)$$

If $F_C > 0$ then the cam and follower are in contact. If $F_C \leq 0$ then separation of cam and follower occurs.

4. Test setup

The experiment setup to observe valvetrain dynamics of Valvetronic VVL is shown in Fig.4. In this work, N42-BMW four stroke petrol engine of 105 HP and 5500 rpm is used. The DOHC valvetrain type is used. The cam profile consists of circular base-nose with circular tangent flanks and RFF. The engine valve mechanism is powered by a 3.5 kW electric motor at 1500 rpm. The VVL is generated during powered engine condition. A 3-phase inverter and variable pulley diameters were used to run the cam shaft at the desired speed. The housing of engine valve mechanism was supported on a heavy steel stand with a concrete base. Fig. 5 shows the DC motor controller of Valvetronic VVL and lift regulation.



(1) 3-phase inverter (2) Electrical motor (4) Variable driven pulley
(4) Cam shaft driver chain (5) Cylinder head (6) Power supply
(7) Step motor controller

Fig. 4: Photograph of test rig layout

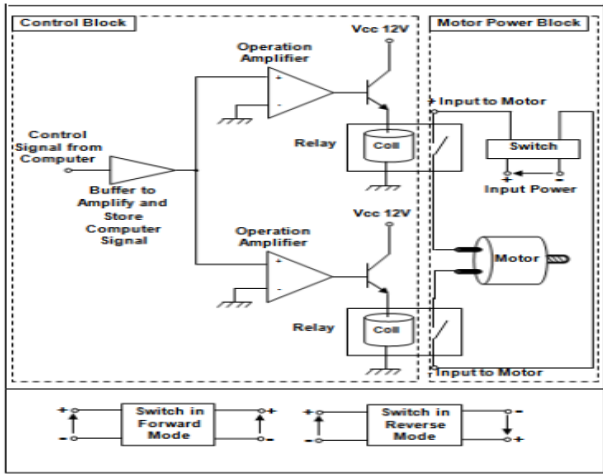


Fig. 5: Block diagram of motor and lift regulation

The acceleration responses for the engine valvetrain were measured by accelerometer in the cam shaft powered conditions. The recorded accelerometer signals were then passed to the data acquisition system with National Instruments LabVIEW program. The center of the valve head plane surface was chosen as a measuring point to minimize possible deviations of the numerical results over one cam revolution (2500 rpm) to the engine speed of 5000 rpm. Fig. 6 shows the schematic experimental setup.

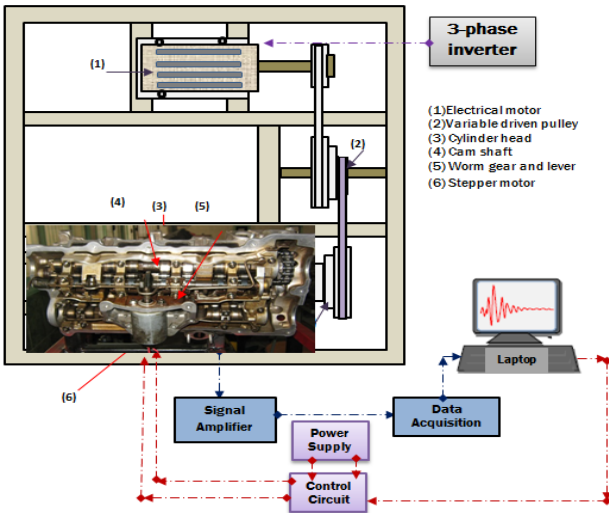


Fig. 6: Schematic of test setup

5. Results and discussions

5.1. Theoretical analysis results

Kinematic and rigid body dynamic analyses are performed to evaluate the mechanism performance after the cam profile design is completed. The smooth polynomial profile of the cam is shown in Fig. 7. The formulated equations describing the kinematics of the valvetrain have been programmed in MATLAB. The main parameters of VVL are shown in Table 1. Fig. 8 shows the follower lift with cam rotation angles for an imposed maximum lift of 10 mm. The profile contains 750 ascents and 750 descents of the follower and 2100 dwells. Figs. 9 and 10 show the follower velocity and acceleration for various cam rotation angles. The acceleration increases at the start of valve open or

closure and it is low when the valve is fully opened or closed. The valve acceleration increases as the speed of cam shaft increases.

Table 1: Key parameters of VVL

Parameter	Notation	Value	Unit
Maximum lift	h_{max}	10	mm
Length of RFF	L_r	35	mm
Friction coeff.	μ	0.15	--
Spring stiffness	K_s	8000	N/m
Cam shaft stiffness	K_{sh}	2.6×10^7	N/m
Valve mass	m_v	0.085	kg
Cam shaft bearing damp coeff.	C_{sh}	0.773	Ns/m
RFF mass	m_r	0.1	kg
Hydraulic valve damp coeff.	C_p	86.5	Ns/m

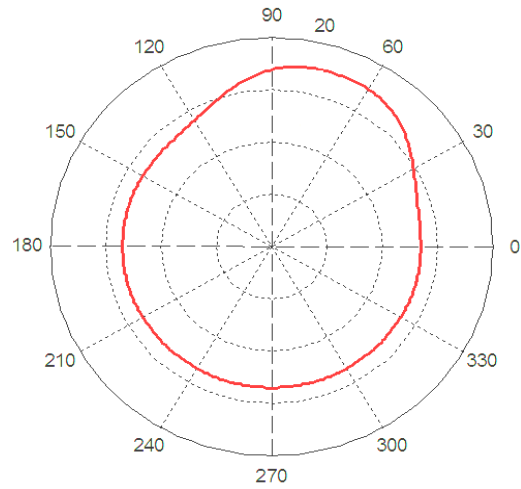


Fig. 7: Smooth polynomial cam profile

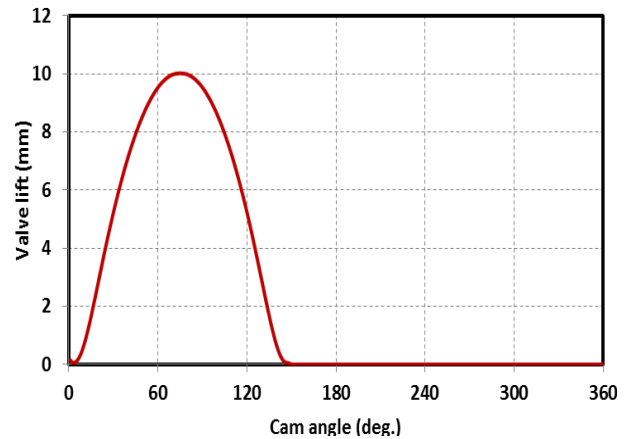


Fig. 8: Displacement of the valve vs. Cam angle

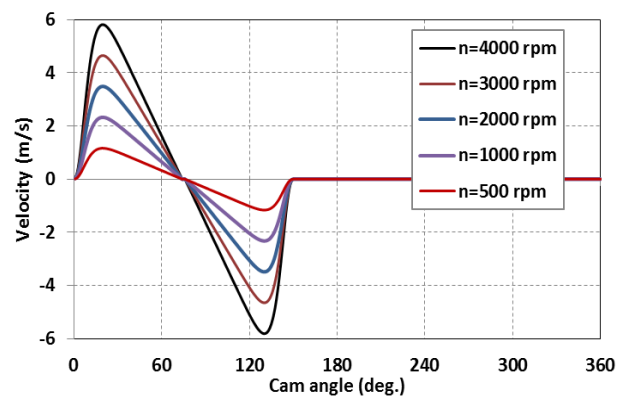


Fig. 9: Velocity of the valve vs. Cam angle

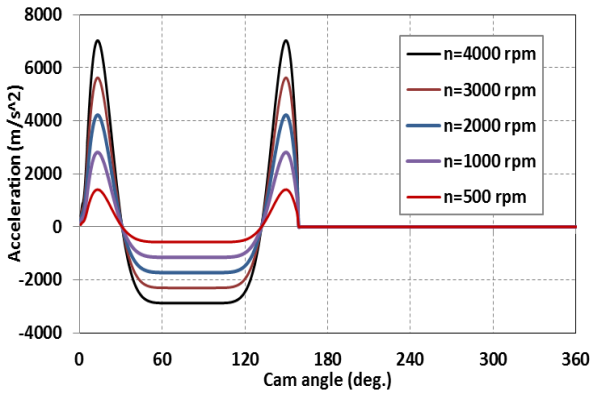


Fig. 10: Acceleration of the valve vs. Cam angle

Fig. 11 shows the valve lift (mm) of VVL for various cam angles (degree) curve at low and high cam shaft speed zones. Fig. 12 shows the contact force between the cam profile and RFF for various cam shaft speeds. The cam profile has a direct effect on the dynamic modeling response of the CVVL system. Figs. 13 and 14 show the cam lift, RFF lift and valve lift for 500 rpm and 2500 rpm. The differences between the lift responses of the valve considering rigid elements and flexible elements are small at low cam shaft speed of 500 rpm. When the cam shaft speed increases to 2500 rpm, the valve bounces during valve closure. Figs. 15 and 16 illustrate the cam, RFF and valve accelerations. The fluctuation of the valve increases at high speeds over 2500 rpm. Fig. 17 illustrates the dynamic contact force between the cam profile and RFF for 500 and 2500 rpm.

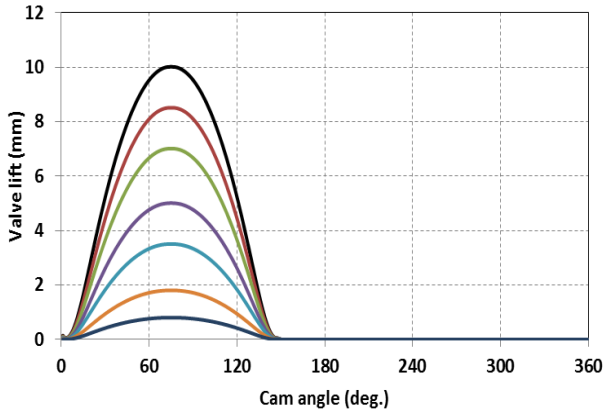


Fig. 11: VVL characteristics

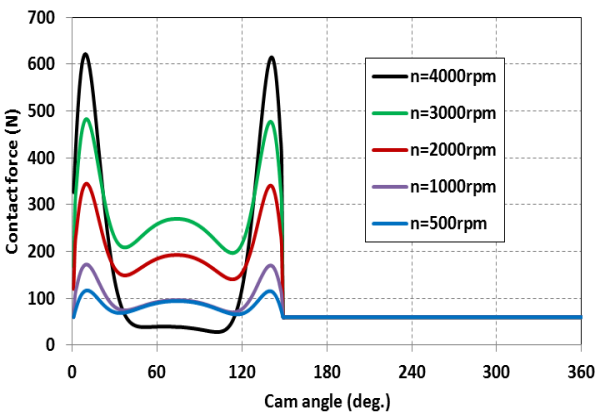


Fig. 12: Contact force between cam and RFF vs. Cam angle

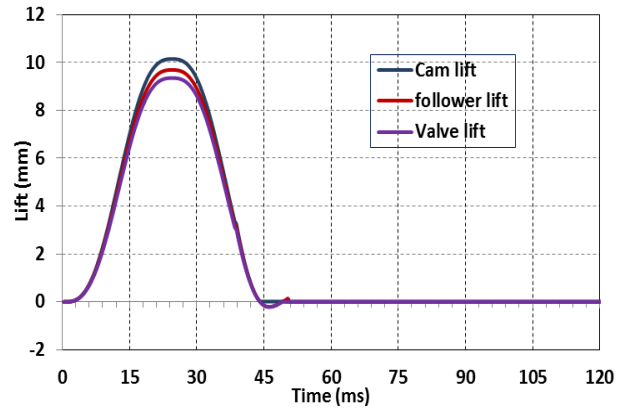


Fig. 13: Valvetrain displacement vs. Time at 500 rpm

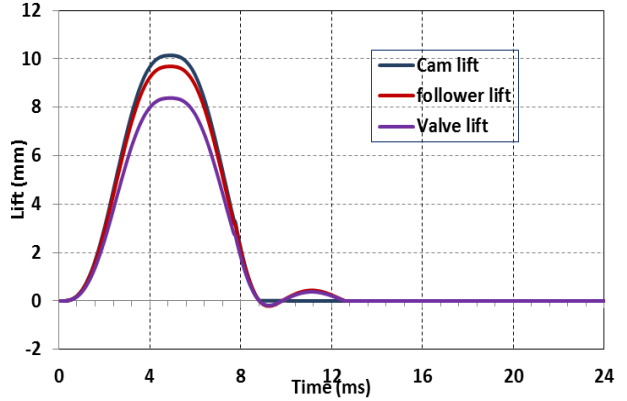


Fig. 14: Valvetrain displacement vs. Time at 2500 rpm

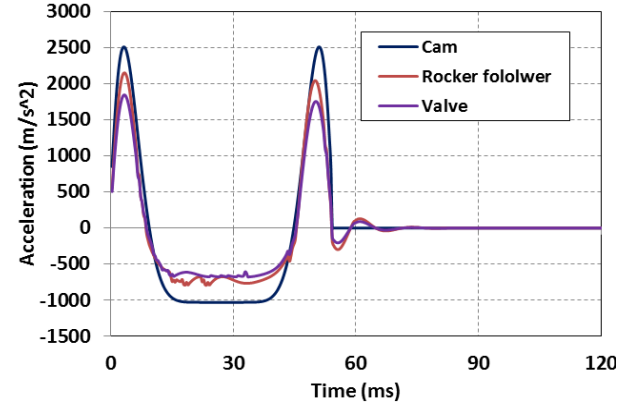


Fig. 15: Valvetrain acceleration vs. Time at 500 rpm

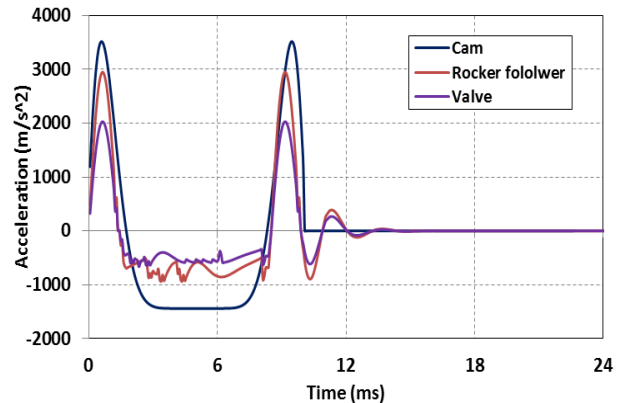


Fig. 16: Valvetrain acceleration vs. Time at 2500 rpm

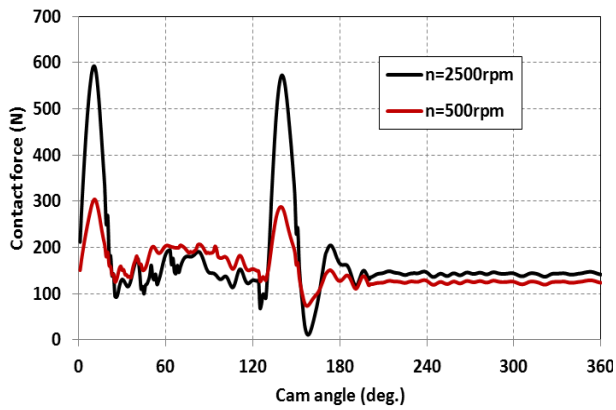


Fig. 17: Dynamic contact force between cam & RFF vs. Cam angle

5.2. Experimental test results

The experimental results have been presented in the form of VVL dynamic characteristics plots of the measured accelerations. The most influencing variables are varied to assess the actual performance of valvetrain mechanism used in this work. Figs. 18 and 19 show the actual valve lift at cam shaft speed of 500 and 2500 rpm respectively. The valve lift can be calculated by double integration of the measured acceleration signals. Figs. 20 and 21 show the actual valve acceleration for different valve lifts at cam shaft speed of 500 and 2500 rpm respectively.

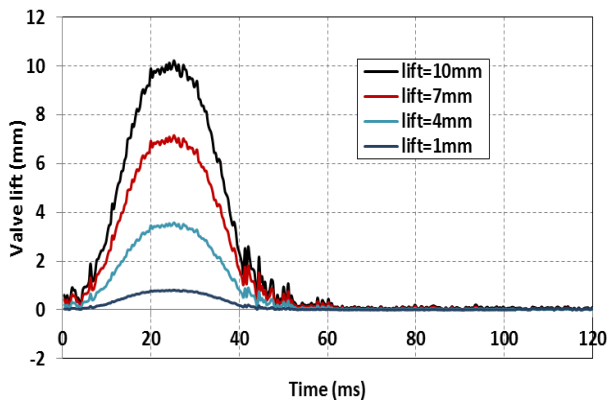


Fig. 18: Valve displacement vs. Time at 500 rpm

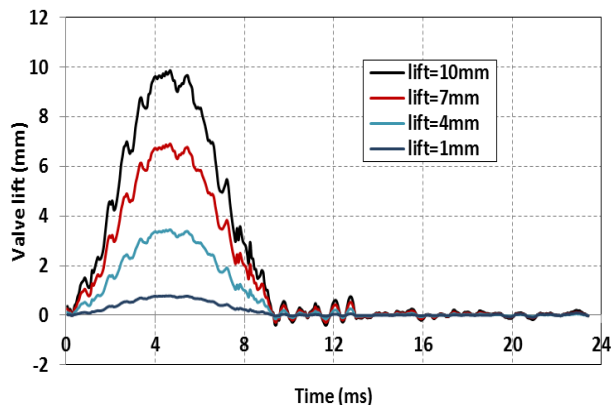


Fig. 19: Valve displacement vs. Time at 2500 rpm

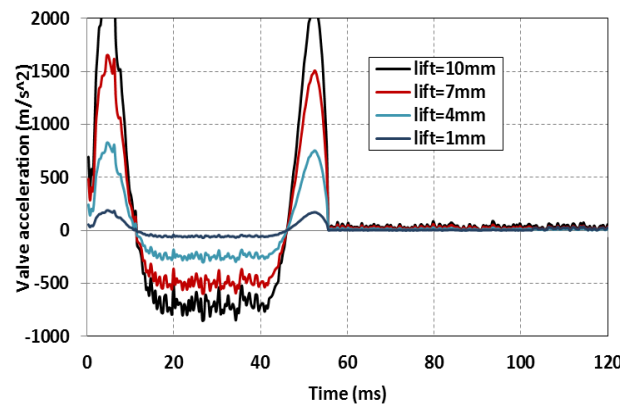


Fig. 20: Valve acceleration vs. Time at 500 rpm

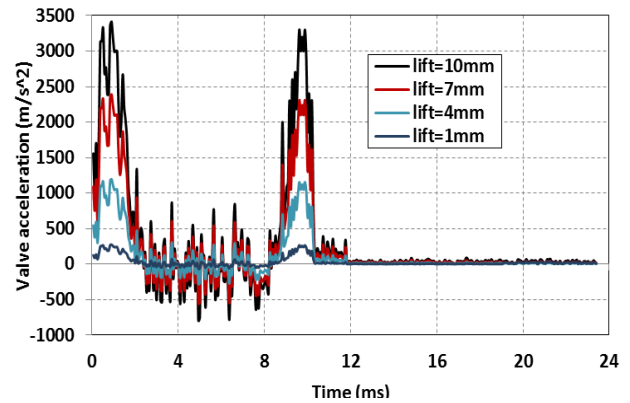


Fig. 21: Valve acceleration vs. Time at 2500 rpm

6. Conclusions

In this paper, one type of VVL is investigated through dynamic analysis and experimental tests using IC engine with a DOHC. The cam shaft speed, cam profile, maximum and minimum valve lift, spring stiffness, VVL masses and friction coefficient between cam and RFF directly affect the system dynamic performance. Each component of the VVL mechanism with polynomial cam profile is then built with their defined geometrical and operational characteristics. Having the whole mechanism is well defined, the kinematic and dynamic analyses are undertaken to calculate the displacements, forces and accelerations of every critical component of the mechanism. Three-degrees of freedom dynamic model is used to evaluate valvetrain characteristics at the maximum engine speed depending on the contact force between the cam and RFF. Testing conducted on the powered cam shaft VVL fixture confirmed the dynamic performance and limited durability of developed N42-BMW VVL system to facilitate the variation in the intake valve lift.

REFERENCES:

- [1] G. Dritsas, P.G. Nikolakopoulos and C.A. Papadopoulos. 2013. Design evaluation of a follower cam with variable valve lift mechanism, *Int. J. Structural Integrity*, 4(1), 7-22. <http://dx.doi.org/10.1108/17579861311303591>.
- [2] J.R. Liu, B. Jin, Y.J. Xie, Y. Chen and Z.T. Weng. 2009. Research on the electro-hydraulic variable valve actuation system based on a three-way proportional reducing valve, *Int. J. Automotive Technology*, 10(1), 27-36, 26-37.

- [3] Y. Kazour, M. Knauf, J. Sinnamon, E. Suh and D. Glueck. 2012. Development of continuously variable valve lift mechanism for improved fuel economy, *SAE Paper 2012-01-0163*. <http://dx.doi.org/10.4271/2012-01-0163>.
- [4] L.C. Sleath and P.G. Leaney. 2013. The use of a two stage dimensional variation analysis model to simulate the action of a hydraulic tappet adjuster in a car engine valvetrain system, *American J. Veh. Design*, 1(2), 36-43.
- [5] T. Fujita, K. Onogawa, S. Kiga and Y. Mae. 2008. Development of innovative variable valve event and lift (VVEL) system, *SAE Paper 2008-01-1349*. <http://dx.doi.org/10.4271/2008-01-1349>.
- [6] E.S. Mohamed. 2012. Modeling and performance evaluation of an electromechanical valve actuator for a camless IC engine, *Int. J. Energy and Environment*, 3(2), 275-294.
- [7] M. Sellnau and E. Rask. 2003. Two-step variable valve actuation for fuel economy, emissions, and performance, *SAE Paper 2003-01-0029*. <http://dx.doi.org/10.4271/2003-01-0029>.
- [8] C. Brüstle and D. Schwarzenthal. 2001. Variocam plus – A highlight of the porsche 911 Turbo Engine, *SAE Paper 2001-01-0245*. <http://dx.doi.org/10.4271/2001-01-0245>.
- [9] R. Flierl, R. Hofman, C. Landerl, T. Melcher and H. Steyer. 2001. The New BMW four cylinder engine with Valvetronic, Part 1: Concept, Design and Construction, *MTZ*, 62(6), 450-463.
- [10] T. Kiran and S.K. Srivastava. 2013. Analysis and simulation of cam follower mechanism using polynomial cam profile, *Int. J. Multidisciplinary and Current Research*, 1(Nov.-Dec.), 211-215.
- [11] M. Anderson, T. Tsao and M. Levin. 1998. Adaptive lift control for a camless electrohydraulic valvetrain, *SAE Paper 981029*. <http://dx.doi.org/10.4271/981029>.
- [12] P. R. Mane and Y.P. Reddy. 2013. Development of variable valve actuation mechanism for multi-cylinder SI engine, *American J. Mechanical Engg.*, 1(5), 131-137. <http://dx.doi.org/10.12691/ajme-1-5-5>.
- [13] M.M. Okarmus and R. Keribar. 2010. Application of a general planar kinematics and multi-body dynamics simulation tool to the analysis of variable valve actuation systems, *SAE Paper 2010-01-1193*. <http://dx.doi.org/10.4271/2010-01-1193>.
- [14] T.H. Muhr and Bender. 1993. New technologies for engine valve springs, *SAE Paper 930912*. <http://dx.doi.org/10.4271/930912>.
- [15] F. Agrell. 2006. *Control of HCCI by Aid of Variable Valve Timings with Specialization in Usage of a Non-Linear Quasi-Static Compensation*, PhD Thesis, KTH, Stockholm, Sweden.